Improved high-resolution GPR imaging and characterization of prehistoric archaeological features by means of attribute analysis

Wenke Zhao [a, b, *], Emanuele Forte [a], Sara Tiziana Levi [c], Michele Pipan [a], Gang Tian [d]

[a] Department of Mathematics and Geosciences, University of Trieste, Italy
[b] The International Centre for Theoretical Physics (ICTP), Italy
[c] Department of Chemical and Geological Sciences, University of Modena and Reggio Emilia, Italy
[d] Department of Earth Sciences, Zhejiang University, China

ARTICLE INFO

Accepted 28 November 2014

Keywords:
GPR
High-resolution geophysics
Prehistoric archaeological remains
Advanced horizon slices
3-D attribute analysis

ABSTRACT

We propose a novel procedure for the analysis and interpretation of Ground-Penetrating Radar (GPR) data from archaeological data and we test the method in challenging conditions at a prehistoric settlement on the Stromboli Island (Italy). The main objective of the proposed procedure is to enhance the GPR capability of identifying and characterizing small-size and geometrically irregular archaeological remains buried beneath rough topographic surface conditions. After the basic GPR processing sequence, including topographic correction using a high-resolution Digital Elevation Model acquired from 3-D Laser Scanner, the procedure encompasses a multi-attribute analysis and iso-attribute surfaces calculation with different volume extraction solutions to emphasize vertical and lateral variations within GPR data cubes. The test was performed in cooperation with the archaeological team to calibrate the results and to provide detailed information about buried targets of potential archaeological interests to plan further excavations. The results gave evidence of localized buried remains and allowed detailed pre-excavation planning. The archaeological excavations validated the results obtained from the GPR survey. The research demonstrates that the proposed GPR procedure enhances the ability to identify and characterize archaeological remains with high accuracy even in complex surface and subsurface conditions. Such logistical situation is very common, particularly in prehistoric sites, which are often characterized by discontinuous, small and irregular targets that cannot be identified by standard processing and analysis strategies.

1. Introduction

Ground-Penetrating Radar (GPR) allows non-invasive high-resolution imaging and characterization of shallow subsurface. It is a geophysical method based on the propagation of electromagnetic (EM) waves in materials where the contrasts of electromagnetic impedance are large enough to allow detection of reflections, diffractions and refractions from targets. GPR techniques have been increasingly used in the last 30 years for the non-destructive and cost-effective imaging and mapping of buried cultural heritage, as GPR datasets offer opportunities to identify archaeological targets in different subsurface conditions with horizontal/vertical resolution not attainable by any other geophysical method (e.g. Vaughan, 1986; Richards, 1998; Pipan et al., 1999, 2001; Leckebusch, 2003; Forte and Pipan, 2008).

True 3-D multi-channel GPR arrays were recently introduced, which allow development of increasingly sophisticated acquisition and processing techniques and further resolution enhancement (Francese et al., 2009; Trinks et al., 2010; Novo et al., 2013). Common offset measurements are nonetheless quicker to perform and to process and are still the most popular data acquisition method. Reflections in 2-D GPR sections obtained along closely-spaced survey lines with sufficient spatial sampling can be correlated, and "pseudo 3-D" volumes (also indicated as "2.5-D" datasets) combining series of parallel and/or intersecting profiles can be obtained allowing a very detailed mapping of both location and spatial extent of targets (Lehmann and Green, 1999; Neubauer, 2001; Leucci and Negri, 2006; Zhao et al., 2013a, 2013b).

* Corresponding author. Department of Mathematics and Geosciences, University of Trieste, Italy.
E-mail address: zwenk@163.com (W. Zhao).

The common way to display 2.5-D radar data is the time-slice technique, in which signal amplitudes are extracted and mapped at constant two way travel-time through the radar data volume (Goodman et al., 1995; Conyers and Leckebusch, 2010). The arrangement of such slices in order of increasing/decreasing depth has a visual format familiar to archaeologists, since it is somehow analogous to the layer stripping and mapping used in excavation. Time slices are actually obtained by extracting 2-D amplitude maps of the radar signals at an individual time sample or by averaging the values within a fixed time window. The latter approach is usually better when the time window length is chosen to average at least one pulse width in order to avoid the bias due to small variations in the transmitted pulse (e.g. Basile et al., 2000; Piro et al., 2003; Conyers, 2010).

Goodman et al. (2006b) proposed an overlay analysis to synthesize reflections located at different travel times in the radar record onto a single composite time slice map, but this analysis is limited to radar signal amplitudes. GPR attribute analysis can produce very precise images of otherwise invisible features, and has therefore been incorporated into GPR data interpretation (Grasmueck, 1996; Senechal et al., 2000; McClymont et al., 2008; Forte et al., 2012), particularly to characterize complex subsurface structures for archaeological prospection (Zhao et al., 2013a, 2013b).

Horizontal slices may not be the best visualization and analysis technique in the case of great subsurface complexity, such as in the case of horizontal slicing planes crossing undulating or irregular reflectors. Accordingly, we propose and test an Advanced Horizon Slices (AHS) technique for improved GPR attribute analysis, specifically aiming at the characterization of buried archaeological remains.

The application of GPR method to archaeological prospection is based on contrasts of physical (electromagnetic) properties and on the recognition of different signatures between man-made and natural features. As a non-destructive technique, GPR is the ideal tool for the investigation of sedimentary geometries, and stratigraphic units (Jol and Smith, 1991; Corbeanu et al., 2001). Facies analysis and sequence-stratigraphic interpretation are widely used for geological characterizations (Neal, 2004; Kostic and Aigner, 2007; Nielsen et al., 2009). On the contrary, it is difficult to track continuous reflections along cultural layers, as the physical contrasts defining the buried cultural heritage are often spatially irregular and not very large. Archaeological remains can be imaged by using slices calculated along geologic horizons, since the relationships usually existing between natural (i.e. sedimentary) and cultural features (Bates, 2005).

The use of 3D visualization techniques based on the AHS is important in archaeological applications after GPR attribute analysis to display complex datasets and allow easier interpretation. In particularly, iso-surfaces are acknowledged as an effective tool for 3-D datasets visualization and analysis, as they reduce the size of the data, allow the identification of each anomaly, and can further speed up the interpretation by implementing semi-automatic procedures. The current iso-surfaces are maps of equal amplitude values across the whole 3-D volume, and significantly improve the overall quality and efficiency of GPR data interpretation (Daniels et al., 1998; Nuzzo et al., 2002; Lualdi and Zanzi, 2004; Leucci and Negri, 2006; Conyers, 2011; Cataldo et al., 2012; Goodman and Piro, 2013).

As for topographic effects, an accurate correction is essential when the survey is taking place on an uneven surface, since buried targets would otherwise no longer be imaged at their true subsurface location. This situation is often met in archaeological prospection (Lehmann and Green, 2000; Heincke et al., 2005; Goodman et al., 2006a). Nonetheless, a correction based on poor topographic data can produce image distortion rather than improving the results.

Various types of topographic solutions emerged in recent years to acquire detailed high-resolution Digital Elevation Model (DEM) or Digital Terrain Model (DTM), with a positioning accuracy in the cm/mm range, such as total stations (Kvamme et al., 2006; McPherron, 2005), aerial-based Lidar measurements (Baltsavias, 1999; Staley et al., 2006), Real Time Kinematic Global Positioning System (RTK-GPS) (Barratt et al., 2000; El-Mowafy, 2000; Schloderer et al., 2011), and terrestrial Laser Scanners (Flood, 2001; Nagihara et al., 2004; Grasmueck and Viggiano, 2007; Hayakawa and Tsumura, 2009).

In this study, we implemented an integrated analysis procedure, which includes high-resolution topographic correction, multi-attribute analysis based on the AHS, and iso-attribute surface calculations with different volume extraction solutions to identify and characterize irregular and mixed archaeological targets from different periods. We tested the procedure in the study of a prehistoric archaeological site located at the San Vincenzo area, Stromboli Island, Italy, which is characterized by rough topographic surface, small and irregular targets and moderate target/background contrast. Due to such complex conditions, San Vincenzo is a challenging site for any geophysical method. We performed there a common offset 2.5-D GPR survey to provide new information about the buried cultural heritage in the 0.5–2 m depth range. The results gave evidence of several localized buried remains characterized by low continuity and allowed a detailed pre-excavation planning. We further validated the GPR interpretation with the results of the first phase of archaeological excavations.

The final goal of this research was to implement and test new GPR data analysis/interpretation strategies to offer a practical and optimized solution to characterize prehistoric remains in complex surface and subsurface conditions, thus improving the overall efficiency of GPR for challenging archaeological applications.

2. Test site

Stromboli is a small island in the Tyrrhenian Sea, off the north coast of Sicily, containing one of the four active volcanoes in Italy. It is one of the seven Aeolian Islands, a volcanic arc located to the North of Sicily. Stromboli is known worldwide for its peculiar, persistent mild explosive (Strombolian) activity, continuously occurring during at least the past 2000 years (Rosi et al., 2000). Massive effusive eruptions occur every few years, and consist of lavas overflowing from the rims of the summit craters, or spilled from fissures opening at the summit cone's flanks (e.g. Chouet et al., 1974; Speranza et al., 2008), while the ashes flow is almost continuous. As a result, the island is constituted by an alternation of ashes, lava flows and loose volcano clastic debris, with a remarkable continuity between the emerged and submerged flanks (Kokelaar and Romagnoli, 1995).

In 1980, the archaeologist found the first evidences of a prehistoric village, in the San Vincenzo's church area, (Fig. 1, north-eastern sector of the island; Cavalier, 1981). The village belongs to Capo Graziano culture and dates back to the Early-Middle Bronze Age (about 2300–1400 B.C.) but the site was inhabited in successive periods and exhibits a superposition of cultural layers, with evidences of archaeological remains that include also Hellenistic to Contemporary periods. Such discovery enriched the exceptional assets of the Aeolian Islands, where the results of many years of research activity by Luigi Bernabò Brea and Madeleine Cavalier helped to define a temporal sequence of cultural levels for all of Southern Italy starting from the Neolithic (Bernabò Brea and Cavalier, 1968, 1980).

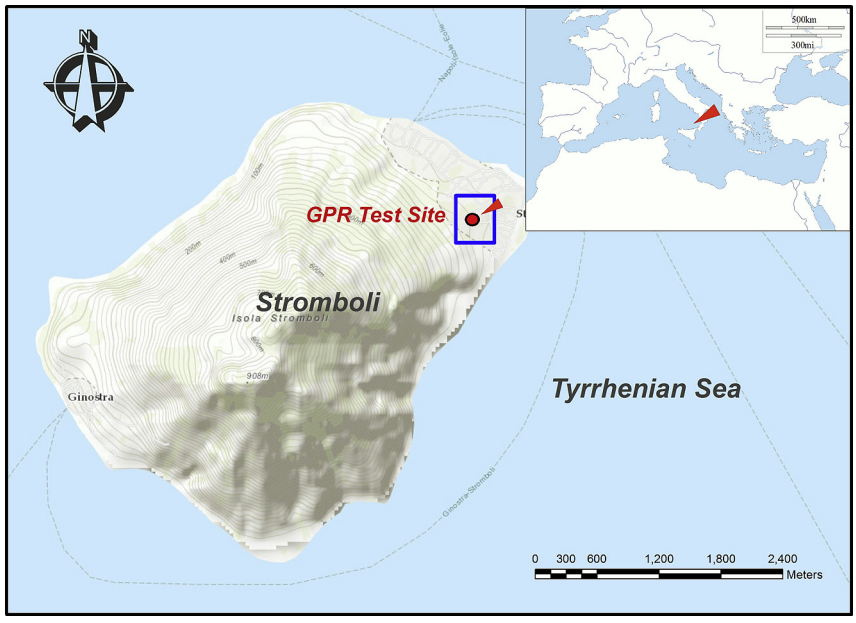

Fig. 1. Location map of the test site San Vincenzo, northeastern Stromboli, Italy.

The village is situated in a strategic position that allows control of the seaways, like an outpost on the north-east part of the Aeolian archipelago, with an open view from the Messina Strait to the Phlegrean Islands. In the Bronze Age, the West Mediterranean routes and markets were controlled by the Minoan civilization and the Minoan rulers looked for new sources of copper and tin in directions that allowed them to navigate visually and that touched the Aeolian Islands.

In the 1980, an area of 16 by 9 m was excavated and a number of structures emerged which were typical remains of rounded huts made of lava rock at the base and wooden structures (unpreserved) as for the upper part of the walls and the roof (Cavalier, 1981). The remains included both parts of the huts and accessories, built with typical techniques from the prehistoric period. Starting from the initial trench and archaeological work, archaeological and geophysical studies resumed from 2009 to identify buried cultural heritage and unveil the remains and the history of ancient Stromboli (Levi et al., 2011).

The choice of San Vincenzo as test-site for the proposed procedure interpretation procedure is due to the complexity of the subsurface conditions (from the geometrical point of view), to the low-contrast of physical properties between buried targets and natural background, to the superposition of different cultural levels and to the overall low signal-to-noise ratio of the GPR data. Such combination of factors offers a challenging opportunity of methodological validation.

3. Methods

3.1. Data acquisition and data processing

The proposed procedure requires 2.5-D or true 3-D GPR datasets. Therefore, we performed a 2.5-D common offset GPR data acquisition with a MalåGeoscience system equipped with 500 MHz central-frequency antennas at the selected test-site (San Vincenzo, Stromboli Island, Italy, Fig. 1). The main objectives of the survey were to test the method and to provide new subsurface information to plan novel archaeological excavations. We carried out the acquisition of 33 profiles along a regular grid with 1 m line spacing and 0.1 m trace distance (Fig. 2). In addition, we obtained high-resolution digital elevation data with a terrestrial Laser Scanner, and correlated the GPR position with the precise DEM model.

The basic GPR processing sequence included: data editing, geometry header definition, DC removal, amplitude analysis, spectral analysis, band-pass filtering, background removal, amplitude recovery, velocity analysis on diffraction hyperbolas, topographic correction (static correction) and f-k migration. According to the

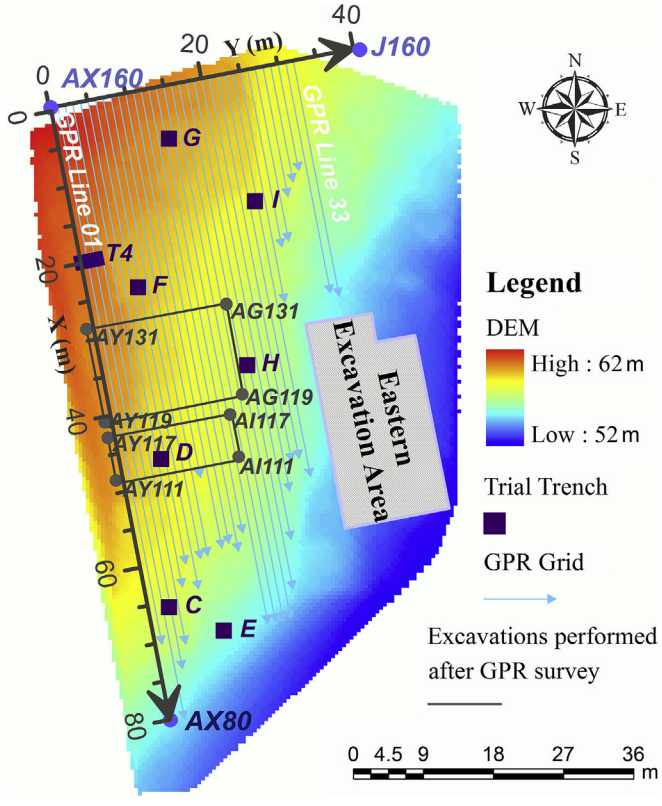

Fig. 2. Digital elevation map, and GPR acquisition grid. Labels containing numbers and letters refer to the archaeological gridding system and are here provided as additional information.

results of the velocity analysis based on diffraction hyperbolas, we estimated a mean 0.12 m/ns EM wave velocity, which was also validated by the trench data.

3.2. Data analysis and interpretation

The preliminary analysis of 2-D data (i.e. GPR sections) is crucial in any GPR data interpretation sequence and in particular, in archaeological applications, to estimate the characteristics of the buried targets. 3-D visualization can successively help mapping the potential archaeological targets assessing their extension, shape, and depth. Assessment of the physical properties of the imaged targets is the final step in the interpretation procedure.

3.2.1. Conventional slices

Horizontal slices (known as "time slices" or "depth slices") are considered a standard practice in GPR archaeological applications, as they allow the remote reconstructions along horizontal levels (Conyers, 2012, 2013). Fig. 3a shows the San Vincenzo 3-D dataset before the topographic correction. Some of the amplitude anomalies in the horizontal slices may correspond to particular remains but the interpretation is not straightforward. Moreover, the signal to noise ratio is rather low and signals are severely distorted due to the extremely irregular surface.

Fig. 3b presents the same data volume after topographic correction: the slices are extracted along levels parallel to the topographic surface. Therefore such slices represent real depths, in a visual format familiar to archaeologists, analogous to the maps of excavation levels. Both type of slices (i.e. before topographic correction, constant two way time; after topographic correction, parallel to topographic surface) are an easy and rapid tool to analyze the anomaly pattern, but limitations still exist when it comes to mapping superimposed complex and irregular targets.

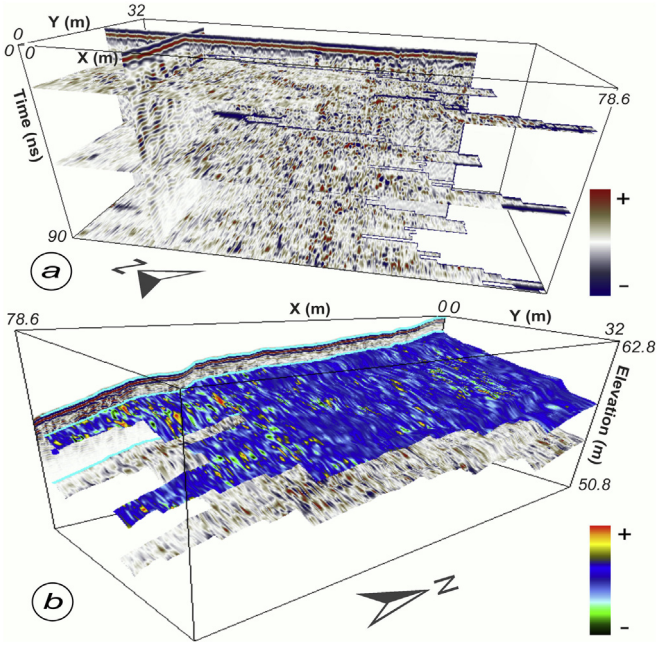

Fig. 3. Conventional GPR slice examples. (a) Horizontal slices calculated on a data volume without any topographic correction (or with perfectly horizontal topography); (b) Depth slices of data volume after topographic correction.

3.2.2. Advanced horizon Slices

We propose and test a novel and improved slicing method to enhance the ability to analyze 3-D GPR archaeological data and to overcome the inherent limitations of conventional slices.

Identification and mapping of archaeological remains can be performed with horizon slices, generated along laminae, bedsets, bounding surfaces and cap layers: the basic idea is that surfaces related to natural, i.e. mainly sedimentary, processes have an often clear correlation with GPR reflections and can be easily tracked across the data volume. Archaeological targets mostly interrupt natural sequences and are found in limited stratigraphic intervals. Therefore, extraction of horizon slices, i.e. along reflectors correlated to sedimentary boundaries, can highlight buried archaeological targets better that standard time-slices.

Fig. 4a shows an example of two horizon slices based on GPR facies analysis and sequence-stratigraphic interpretation. All of such slices can be shifted up and down to explore the data volume or can be used to calculate mean values centered on the original slices, thus allowing a better understanding of the main subsurface structures as Fig. 4b shows.

3.2.3. Multi-attribute analysis

GPR attribute analysis can produce accurate images of otherwise invisible features, particular in archaeological prospection of complex subsurface structures, as discussed in detail by Zhao et al. (2013a). In this study, we use attributes such as instantaneous amplitude, energy, a two-step attribute (similarity of the energy)

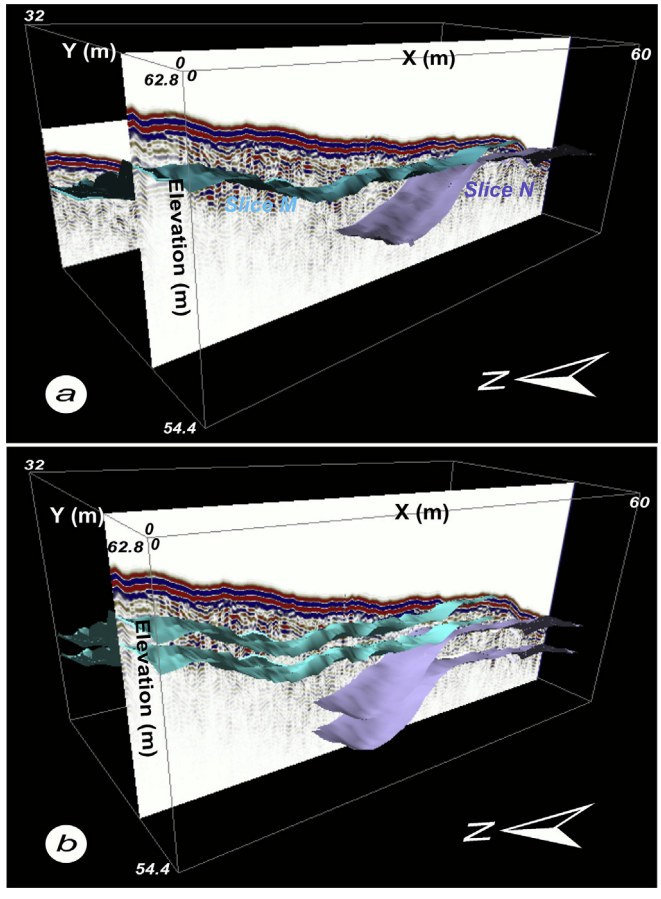

Fig. 4. Advanced horizon slice examples. (a) Slice 'M' (cyan) and Slice 'N' (light blue) based on GPR facies analysis and sequence-stratigraphic interpretation; (b) Two sets of slices, parallel to Slices 'M' and 'N', respectively. (For interpretation of the references to color in this figure legend, the reader is referred to the web version of this article.)

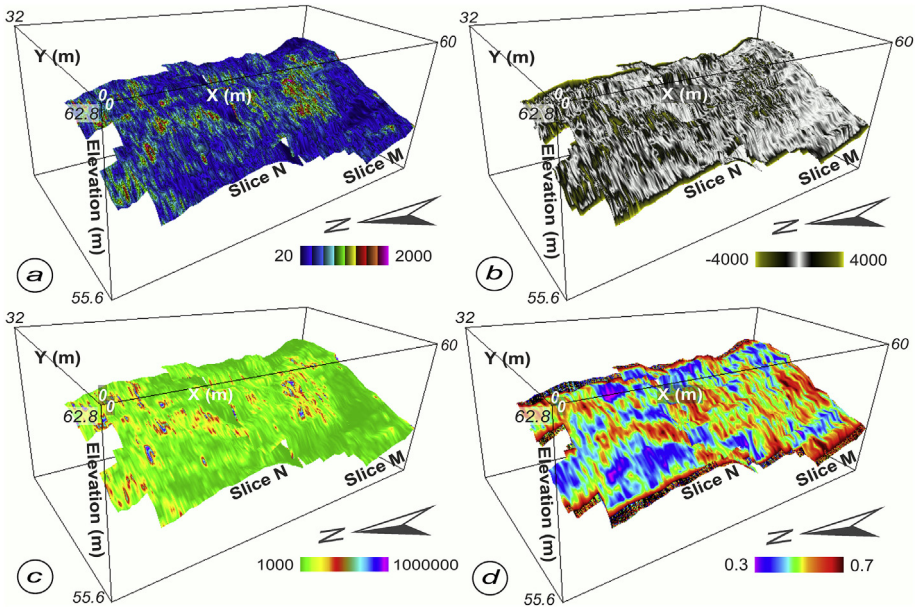

Fig. 5. Comparison of attributes calculated on Slices 'M' and 'N'. (a) Instantaneous amplitude; (b) Edge enhancing filter; (c) Energy; (d) Similarity calculated on the energy volume.

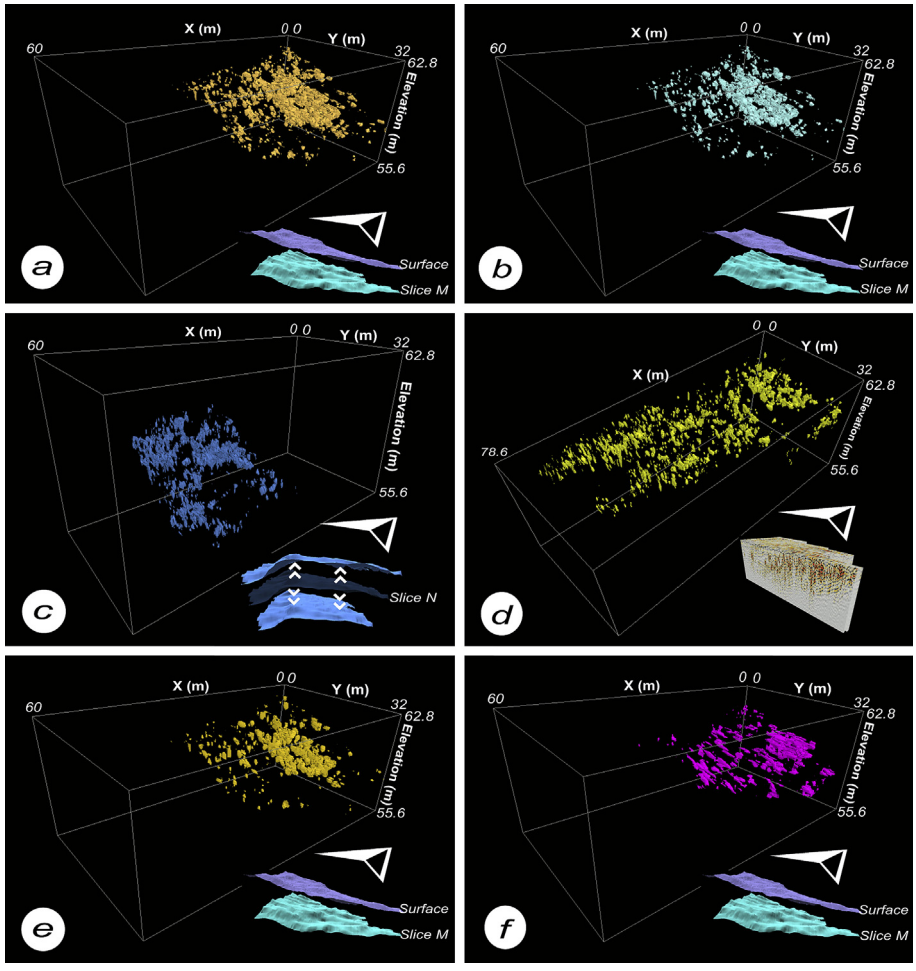

Fig. 6. Comparison between different iso-attribute surfaces. (a) Iso-amplitude surface with a threshold value at 80% of the maximum instantaneous amplitude based on the volume between the topographic surface and Slice 'M'; (b) Iso-amplitude surface with a threshold value at 90% of the maximum instantaneous amplitude based on the volume between the topographic surface and Slice 'M'; (c) Iso-amplitude surface with a threshold value at 80% of the maximum instantaneous amplitude based on the volume formed by Slice 'N' shifted up and down; (d) Iso-amplitude surface with a threshold value at 80% of the maximum instantaneous amplitude based on the volume formed by the whole 3-D GPR data without topographic correction; (e) Iso-energy surface with a threshold value at 80% of the maximum energy based on the volume between the topographic surface and Slice 'M'; (f) Iso-similarity (calculated on the energy attribute) surface with a value equal to 0.68 based on the volume between the topographic surface and Slice 'M'.

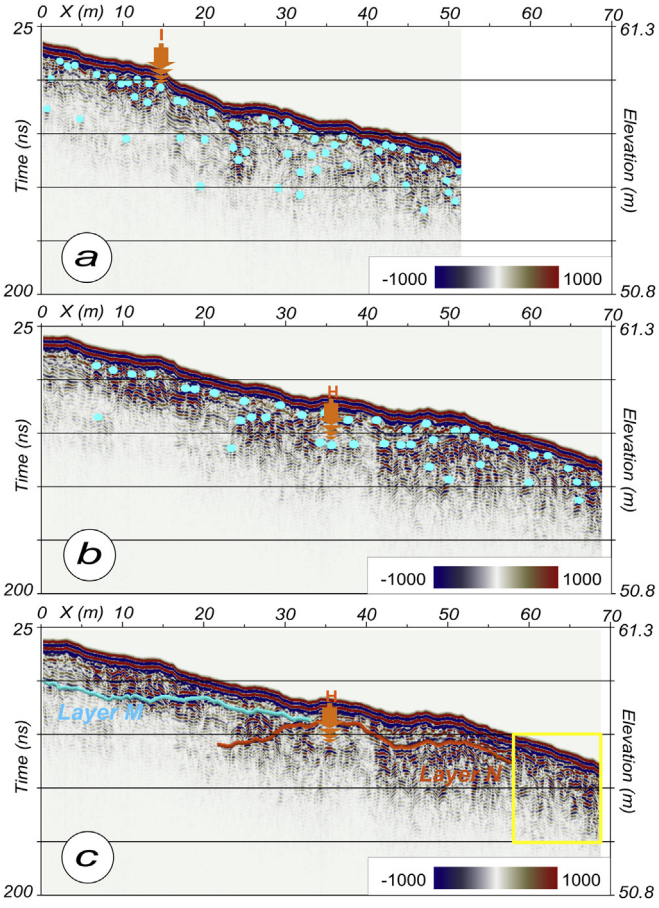

Fig. 7. Example of 2-D processed GPR amplitude profiles. (a) Line 21; (b) Line 26; (c) Line 26 with layer interpretation superimposed. Cyan circles indicate subsurface features potentially linked to archaeological targets. Building materials of the Classical period were found in Trench I, buried at about 0.4 m, and remnants of the Bronze Age were found in Trench H, buried at about 1.5 m. (For interpretation of the references to color in this figure legend, the reader is referred to the web version of this article.)

and edge detection techniques to better understand the subsurface features located close to Slice 'M' and Slice 'N' (Fig. 5).

Instantaneous attributes are based on complex signal theory, whose original application was the mathematical treatment of amplitude-modulated and frequency-modulated transmission (White, 1991). Instantaneous amplitude variations on the selected data volume mainly represent impedance contrasts. The basic principle of edge detection techniques is that a discontinuity can be interpreted as a sharp lateral phase variation and therefore can be detected as an "edge" (Luo et al., 1996; Marfurt et al., 2002). We apply an edge detection technique to identify lateral signal variations and discontinuities, which can be both related to the archaeological remains. Energy is a measure of reflectivity in a specified time-gate. Such attribute can only be positive (like the reflection strength) and can be useful to emphasize low or irregular amplitude reflections. It is a simple and robust attribute to map 3-D GPR structures with a relative low level of subjectivity. Moreover, similarity is a measurement of coherency that expresses how much two or more trace segments look alike (De Rooij and Tingdahl, 2002).

Further mathematical details and a more exhaustive description of the attributes calculation for GPR data can be found in Forte et al. (2012).

3.2.4. Iso-attribute surfaces

The attribute maps based on advanced horizon slices can improve the ability to display complex data; however, they cannot provide an instantaneous view of the complete data-volume. With faster and more powerful computers, iso-surface calculations can make the subsurface structures more visible, particularly in the case of laterally discontinuous structures.

Before the extraction of iso-surfaces, we define the following sub-volumes for the calculation: the volume between different horizon slices; the volume formed by one horizon slice shifted up and down; and the whole data volume. These three cases are all reported in Fig. 6, where Fig. 6a, b, e, f show the volume between the topographic surface and Slice 'M', Fig. 6c shows the volume formed by Slice 'N' shifted up and down, and Fig. 6d shows the calculation made considering the whole 3-D GPR data without topographic correction.

In addition, it is possible to display any iso-surface showing values between 0 and 100% of the maximum within the selected volume. The higher threshold value is selected, the stronger reflections are displayed. Fig. 6a and b shows 80% and 90% threshold values of the maximum instantaneous amplitude respectively. Relatively strong continuous reflections are visible on the 3-D volumes, and the shape and the size of the anomalies suggest that they can be related to the presence of archaeological remains.

Besides the iso-amplitude surface, iso-energy, and iso-similarity (calculated on the energy attribute) surfaces were also created and visualized (Fig. 6e, and f). Several different attribute data volumes can be visualized as iso-attribute surfaces, such as iso-frequency surface and iso-texture surface. The iso-attribute surfaces share the common characteristics of considerably reducing the size of the data while at the same time enhancing the ratio between useful information and total amount of data.

4. Results

4.1. 2-D profiles

The processed GPR sections 21 and 26, were selected from the 33 profiles of the 2.5-D dataset because they exhibit typical characteristics of the data from the proposed archaeological test-site. Moreover, they share common characteristics with several archaeological sites where the subsurface is characterized by geological layers with complicated morphology and archaeological targets of different size and shape with quite low lateral continuity. Fig. 7 shows the two profiles after the application of the processing sequence illustrated in Section 3.1.

Several high amplitude GPR reflections/diffractions are indicated by cyan circles, which may be associated with potential archaeological structures. Since the test-site is located on the flank of the active Stromboli Volcano and has a soil composed by pyroclastic products with local alluvial sediments and lava blocks, the environment is very complicated for the GPR exploration since the texture is quite chaotic and the archaeological structures are essentially made by blocks that have physical properties similar to those of surrounding materials (natural background). In addition, the location of two trial trenches 'I' and 'H' is also indicated: building materials of the Classical Period were found in Trench I, buried at about 0.4 m, while remnants of the Bronze Age were found in Trench H, buried at about 1.5 m (Cavalier, 1981). The reflections observed in GPR profiles are consistent with the trench data.

Layers 'M' and 'N', are continuous on large portions of the investigated area and are associated to volcanic ash layers and tracked with facies analysis and sequence-stratigraphic interpretation on all the lines. Slices 'M' and 'N' are obtained by combining the data across the whole 3-D GPR volume. By using the trench information, there is considerable evidence that the reflections close to layer 'M' are indicators of archaeological remnants of the

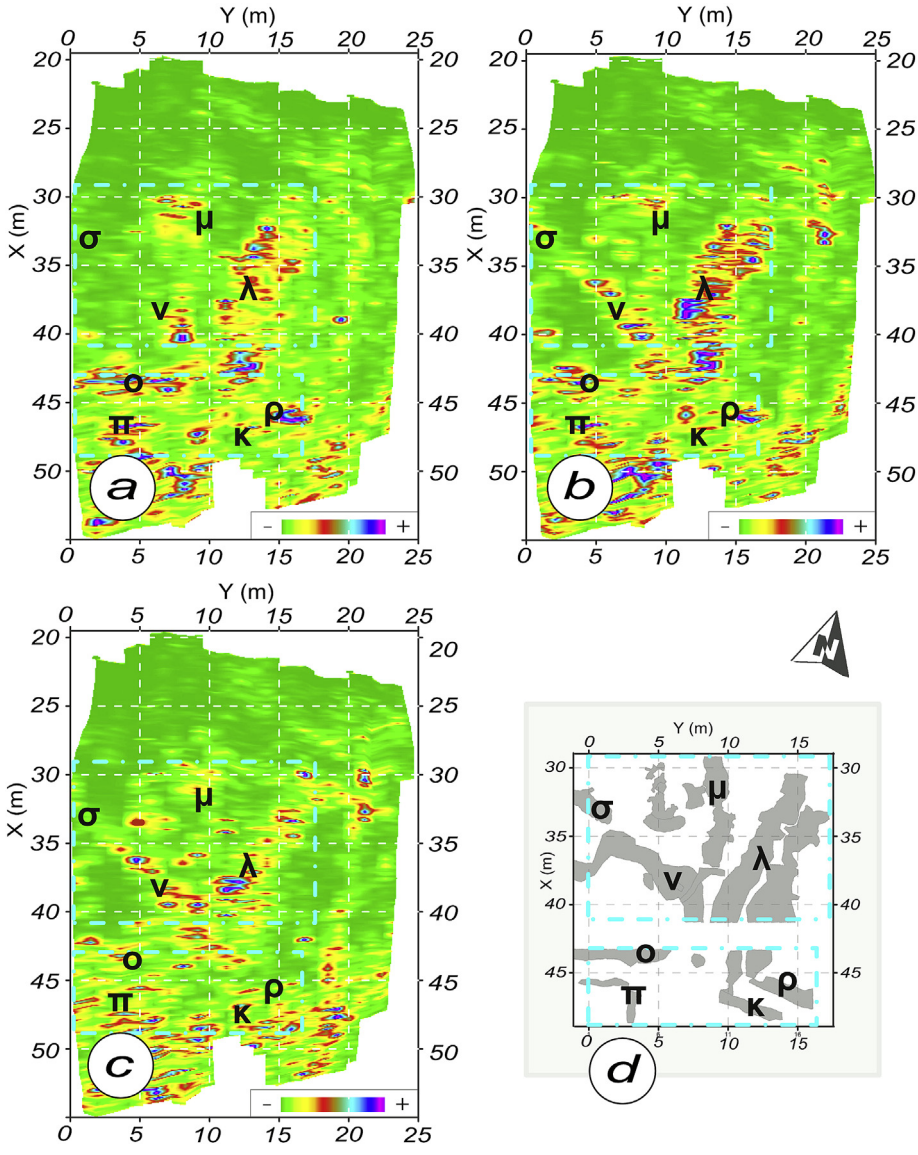

Fig. 8. Comparison between GPR energy attribute maps calculated based on the horizon slice 'N' and detailed excavation map. (a) Slice 'N'; (b) Slice 'N' shifted down 5 ns; (c) Slice 'N' shifted down 10 ns; (d) The location and extent of prehistoric archaeological structures.

Classical period, while reflections below layer 'N' can be rather related to archaeological structures of the Bronze Age, as indicated by the calibration with the trench data. In this case, there are overlaps in the vicinity of 25 m from the beginning of the GPR lines, and there are also areas which are not tracked (as the yellow rectangle on Fig. 7c shows), where the continuity and the characteristics of GPR facies are not so clear. Therefore, it could be argued that the archaeological remains of different historic periods can be mapped individually within the data volume, by considering such horizon pattern.

4.2. 3-D results

The main objective of the archaeological work at the test site was to locate pre-Classical, Bronze Age remains: we therefore focused on the reconstruction of subsurface structures located below Slice 'N'. We started such analysis by calculating the energy attribute to map the possible archaeological features in terms of extension and shape, and to infer the level of contrast between target and background, as this attribute is a simple and robust way to map 3-D GPR structures with a relative low level of subjectivity.

Fig. 8 shows GPR energy attribute maps and a detailed excavation map with several irregular and often interconnected prehistoric structures, discovered and validated by the archaeological excavation after the GPR survey results. From these pictures we can see that the general trends highlighted by GPR maps are consistent with the excavations, except for some local anomalies, because of the different depths of GPR targets. Correspondence between GPR anomalies and excavations is indicated by the Greek letters λ, μ, ν, ο, π, κ, ρ, and σ in Fig. 8.

This slicing method just provides a general plan view of the most probable archaeological features, which is the primary result required by archaeological teams.

In order to reconstruct the real position of subsurface structures and to properly image their size and shape, we use iso-amplitude surface analysis based on different data volumes (Fig. 9). The threshold values of the maximum instantaneous amplitude were all set to 80%. Yellow iso-amplitude surfaces are extracted from the volume limited by the ground surface and Slice 'M', while cyan iso-

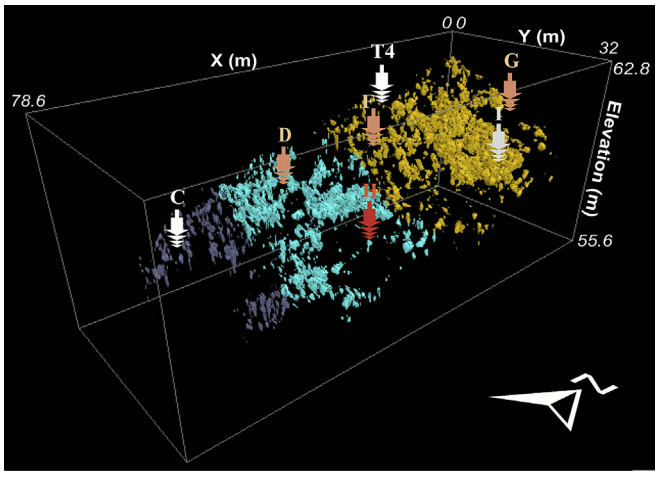

Fig. 9. Examples of iso-amplitude surfaces from the San Vincenzo test-site. Yellow iso-amplitude surfaces represent archaeological remnants of the Classical period; cyan iso-amplitude surfaces represent archaeological remnants of the Bronze Age; and pastel blue iso-amplitude surfaces are additional potential archaeological target not correlated and dated by any trench. Capital letters C, D, E, F, H, I and T4 represent the location of six trenches. C, T4: no relevant archaeological remains; D, F, G: few archaeological fragments; I: materials of the Classical period, buried at about 40 cm; H: remnants of the Bronze Age, buried at about 1.5 m. (For interpretation of the references to color in this figure legend, the reader is referred to the web version of this article.)

amplitude surfaces are extracted from the volume obtained moving the Slice 'N' down for 10 ns below its original position. We adopted such strategy because the most promising prehistoric targets are expected at average depths below Slice 'N'. In addition, pastel-blue iso-amplitude surfaces are extracted from the whole volume without considering any layer discussed in Section 4.1. Some superimposed archaeological remnants of different periods in the vicinity of 25 m (see Fig. 7c), are displayed separately and can be identified in the iso-surfaces of Fig. 9. The shape and extent of the structures referred to the Bronze Age are consistent with the excavations performed after the geophysical surveys and based on the GPR results (Fig. 8d). Potential archaeological targets are also shown in Fig. 9 without interpretation about their age, due to the lack of lateral continuity of GPR facies and trench data. Moreover, several different trench results, reported in Fig. 9 show a remarkable correlation between GPR signal and the actual subsurface structures. Results combined in Fig. 9 can be analyzed by separating the sub-volumes and can be in this way intuitively interpreted by archaeologists and non-geophysical end users.

5. Discussions and conclusions

The key elements of the proposed GPR interpretation procedure are high-resolution (centimeter accuracy) topographic correction, multi-attribute analysis based on advanced horizon slices, and iso-attribute surface visualization and analysis with different volume extraction solutions.

The AHS technique remarkably improves the visual detection of targets and optimizes the level of information useful for archaeologists. Such enhancement in the interpretation performance is primarily due to the improvement in the visualization of natural (i.e. sedimentary) surfaces obtained by moving from the standard time/depth-slice concept to the advanced horizon slice one. Surfaces that accurately reproduce the sedimentary features allow easier identification of anomalies that are related to targets linked to human activities. Such targets have clear relationships with the sedimentary levels and can therefore be isolated, subdivided and classified by analyzing AHS and iso-surfaces. Such results cannot be achieved in complicated subsurface conditions by using the standard slicing techniques. Additional benefits come from the multi-attribute component, which introduces enhanced capability of target detection even in noisy and low-contrast conditions. Attributes that emphasize reflection shape, dip, continuity and phase relationships successfully integrate those more sensitive to amplitude variations and allow in this way tracking of weak signals in noisy background and extension of the interpretation to the maximum possible depth. Interaction with the archaeological team is crucial in all of the phases of the interpretation, from definition of the slices to the correlation of GPR signals and the archaeological targets. In particular, information from boreholes, trenches, test pits has to be included from the initial phase in the analysis procedure and not limited to the calibration.

Attributes provide quantitative information as well as a powerful and intuitive tool for improved data interpretation. Based on the general trend in seismic data interpretation, with specific reference to the developments in hydrocarbon exploration, and on the links between GPR and seismic reflection techniques, increasing interest and research effort can be expected towards a more detailed and quantitative interpretation of GPR data also relying on attribute-based analysis flows. Attribute analysis can promote a major advancement in the application of GPR technology to archaeology, also as a consequence of advances in 3-D visualization technology. Iso-attribute surfaces can emphasize temporal and spatial variations in GPR data volumes as indicated by the results of the present study and test. The optimum choice of surfaces and combinations of attributes is actually an open field for geophysical applications to archaeology because is primarily based on the relationships among GPR signals, natural discontinuities and buried archaeological targets. Such relationships are strongly site dependent.

The site selected to test the procedure (San Vincenzo - Stromboli) is a typical prehistoric settlement and is characterized by rough topographic surface, low contrast between target and background, archaeological targets of limited extension and irregular shape (in plan view). Moreover, there are several superimposed and sometimes interconnected structures, which are related to various periods having totally different archaeological meaning. The method was therefore tested in very challenging conditions.

The application of the proposed procedure, combined with the limited available trench data, allowed the identification and mapping of archaeological remains of different historic periods with iso-attribute surfaces. The extensive archaeological excavations, performed by following the indications provided by GPR, validated the accuracy of the proposed analysis and interpretation techniques.

In synthesis, the proposed interpretation strategy can enhance the ability to identify and map archaeological remains by means of GPR, and can be a powerful exploration tool for non-invasive archaeological prospection.

Acknowledgments

We gratefully acknowledge the support of the International Centre for Theoretical Physics (ICTP, Trieste, Italy) Training on Research in Italian Laboratories (TRIL) programme, which sponsored the scholarship of the first author. We also thank dGB Earth Sciences for providing OpendTect open source seismic data analysis software. The authors thank the archaeological team members Daniele Pantano, Andrea Di Renzoni and Francesco Sartor for their help during the data acquisition and for sharing the archaeological GIS and DEM. We further thank Simone Pillon for help in combining GPR and DEM data, and two anonymous reviewers for providing thoughtful and useful suggestions.

References

Baltsavias, E.P., 1999. Airborne laser scanning: existing systems and firms and other resources. J. Photogramm. Remote Sens. 54, 164–198.

Barratt, G., Gaffney, V., Goodchild, H., Wilkes, S., 2000. Survey at Wroxeter using carrier phase, differential GPS surveying techniques. Archaeol. Prospect. 7 (2), 133–143.

Basile, V., Carrozzo, M.T., Negri, S., Nuzzo, L., Quarta, T., Villani, A.V., 2000. A ground-penetrating radar survey for archaeological investigations in an urban area (Lecce, Italy). J. Appl. Geophys. 44 (1), 15–32.

Bates, R., 2005. Ground penetrating radar in sediments. Archaeol. Prospect. 12, 203–204.

Bernabò Brea, L., Cavalier, M., 1968. Meligunìs Lipàra III. Stazioni preistoriche delle isole Panarea. Salina e Stromboli, Palermo.

Bernabò Brea, L., Cavalier, M., 1980. Meligunìs Lipàra IV. L'Acropoli di Lipari nella preistoria, Palermo.

Cataldo, R., D'Agostino, D., Leucci, G., 2012. Insights into the buried archaeological remains at the Duomo of Lecce (Italy) using ground-penetrating radar surveys. Archaeol. Prospect. 19 (3), 157–165.

Cavalier, M., 1981. Stromboli: villaggio preistorico di S. Vincenzo. Scavi Giugno 1980. Sicil. Archeol. Trapani 14 (46–47), 27–54.

Chouet, B., Hamisevicz, N., McGetchin, T.R., 1974. Photoballistics of volcanic jet activity at Stromboli, Italy. J. Geophys. Res. 79 (32), 4961–4976.

Conyers, L.B., 2010. Ground-penetrating radar for anthropological research. Antiquity 84, 1–11.

Conyers, L.B., Leckebusch, J., 2010. Geophysical archaeology research agendas for the future: some ground-penetrating radar examples. Archaeol. Prospect. 17, 117–123.

Conyers, L.B., 2011. Discovery, mapping and interpretation of buried cultural resources non-invasively with ground-penetrating radar. J. Geophys. Eng. 8, S13–S22.

Conyers, L.B., 2012. Interpreting Ground-penetrating Radar for Archaeology. Left Coast Press, Walnut Creek, California.

Conyers, L.B., 2013. Ground-penetrating Radar for Archaeology, third ed. Rowman and Littlefield Publishers, Alta Mira Press, Latham, Maryland.

Corbeanu, R.M., Soegaard, K., Szerbiak, R.B., Thurmond, J.B., McMechan, G.A., Wang, D., Snelgrove, S.H., Forster, C.B., Menitove, A., 2001. Detailed internal architecture of a fluvial channel sandstone determined from outcrop, cores and 3-D ground-penetrating radar: example from the mid-Cretaceous Ferron Sandstone, east-central Utah. AAPG Bull. 85, 1583–1608.

Daniels, J.J., Brower, J., Baumgartner, F., 1998. High resolution GPR at Brookhaven national laboratory to delineate complex subsurface targets. J. Environ. Eng. Geophys. 3 (1), 1–5.

De Rooij, M., Tingdahl, K., 2002. Meta–attributes the key to multivolume, multi-attribute interpretation. Lead. Edge 21 (10), 1050–1053.

El-Mowafy, A., 2000. Performance analysis of the RTK technique in an urban environment. Aust. Surv. 45 (1), 47–54.

Flood, M., 2001. Laser altimetry: from science to commercial lidar mapping. Photogramm. Eng. Remote Sens. 67, 1209–1217.

Forte, E., Pipan, M., 2008. Integrated seismic tomography and ground-penetrating radar (GPR) for the high-resolution study of burial mounds (tumuli). J. Archaeol. Sci. 35, 2614–2623.

Forte, E., Pipan, M., Casabianca, D., Di Cuia, R., Riva, A., 2012. Imaging and characterization of a carbonate hydrocarbon reservoir analogue using GPR attributes. J. Appl. Geophys. 81, 76–87.

Francese, R.,G., Finzi, E., Morelli, G., 2009. 3-D high-resolution multi-channel radar investigation of a Roman village in Northern Italy. J. Appl. Geophys. 67, 44–51.

Goodman, D., Nishimura, Y., Hongo, H., Higashi, N., 2006a. Correcting for topography and the tilt of ground-penetrating radar antennae. Archaeol. Prospect. 13, 157–161.

Goodman, D., Nishimura, Y., Rogers, J.D., 1995. GPR time-slices in archaeological prospection. Archaeol. Prospect. 2, 85–89.

Goodman, D., Piro, S., 2013. GPR Remote Sensing in Archaeology. Springer, Verlag Berlin Heidelberg.

Goodman, D., Steinberg, J., Damiata, B., Nishimura, Y., Schneider, K., Hiromichi, H., Higashi, N., 2006b. GPR overlay analysis for archaeological prospection. In: Proceedings of the 11th International Conference on Ground Penetrating Radar.

Grasmueck, M., 1996. 3-D ground-penetrating radar applied to fracture imaging in gneiss. Geophysics 61 (4), 1050–1064.

Grasmueck, M., Viggiano, D.A., 2007. Integration of ground-penetrating radar and laser position sensors for real-time 3-D data fusion. IEEE Trans. Geosci. Remote Sens. 45 (1), 130–137.

Hayakawa, Y.S., Tsumura, H.O., 2009. Utilization of laser range finder and differential GPS for high-resolution topographic measurement at Hacitugrul Tepe, Turkey. Geoarchaeology 24 (2), 176–190.

Heincke, B., Green, A.G., Kruk, J.V.D., Horstmeyer, H., 2005. Acquisition and processing strategies for 3D georadar surveying a region characterized by rugged topography. Geophysics 70 (6), K53–K61.

Jol, H.M., Smith, D.G., 1991. Ground penetrating radar of northern lacustrine deltas. Can. J. Earth Sci. 28 (12), 1939–1947.

Kokelaar, P., Romagnoli, C., 1995. Sector collapse, sedimentation and clast population evolution at an active island-arc volcano: Stromboli, Italy. Bull. Volcanol. 57 (4), 240–262.

Kostic, B., Aigner, T., 2007. Sedimentary architecture and 3D ground-penetrating radar analysis of gravelly meandering river deposits (Neckar Valley, SW Germany). Sedimentology 54 (4), 789–808.

Kvamme, K.L., Ernenwein, E.G., Markussen, C.J., 2006. Robotic total station for microtopographic mapping: an example from the northern great plains. Archaeol. Prospect. 13 (2), 91–102.

Leckebusch, J., 2003. Ground-penetrating radar: a modern three-dimensional prospection method. Archaeol. Prospect. 10, 213–240.

Lehmann, F., Green, A.G., 1999. Semiautomated georadar data acquisition in three dimensions. Geophysics 64 (3), 719–731.

Lehmann, F., Green, A.G., 2000. Topographic migration of georadar data: implications for acquisition and processing. Geophysics 65 (3), 836–848.

Leucci, G., Negri, S., 2006. Use of ground penetrating radar to map subsurface archaeological features in an urban area. J. Archaeol. Sci. 33, 502–512.

Levi, S.T., Bettelli, M., Di Renzoni, A., Ferranti, F., Martinelli, M.C., 2011. 3500 anni fa sotto il vulcano. La ripresa delle indagini nel villaggio protostorico di Stromboli. Riv. Sci. Preistoriche LXI, 159–174.

Lualdi, M., Zanzi, L., 2004. 2D and 3D experiments to explore the potential benefit of GPR investigations in planning the mining activity of a limestone quarry. In: IEEE: Proceedings of the Tenth International Conference on Ground Penetrating Radar, pp. 613–616.

Luo, Y., Higgs, W.G., Kowalik, W.S., 1996. Edge detection and stratigraphic analysis using 3D seismic data. Seg. Expand. Abstr. 324–327.

Marfurt, K.J., Duncan, W.S., Constance, P., 2002. Comparison of 3-D edge detection seismic attributes to Vinton Dome Louisiana. Seg. Expand. Abstr. 21, 577–580.

McClymont, A.F., Green, A.G., Streich, R., Horstmeyer, H., Tronicke, J., Nobes, D.C., Pettinga, J., Campbell, J., Langridge, R., 2008. Visualization of active faults using geometric attributes of 3D GPR data: an example from the Alpine Fault zone, New Zealand. Geophysics 73 (2), B11–B23.

McPherron, S.J., 2005. Artifact orientations and site formation processes from total station proveniences. J. Archaeol. Sci. 32 (7), 1003–1014.

Nagihara, S., Mulligan, K.R., Xiong, W., 2004. Use of a three-dimensional laser scanner to digitally capture the topography of sand dunes in high spatial resolution. Earth Surf. Process. Landf. 29, 391–398.

Neal, A., 2004. Ground-penetrating radar and its use in sedimentology: principles, problems and progress. Earth-sci. Rev. 66 (3), 261–330.

Neubauer, W., 2001. Images of the invisible-prospection methods for the documentation of threatened archaeological sites. Naturwissenschaften 88 (1), 13–24.

Nielsen, L., Brockdorff, A., Bjerager, M., Surlyk, F., 2009. Three-dimensional architecture and development of Danian bryozoan mounds at Limhamn, south-west Sweden, using ground-penetrating radar. Sedimentology 56, 695–708.

Novo, A., Leckebusch, J., Goodman, D., Morelli, G., Piro, S., Catanzariti, G., 2013. Advances in GPR imaging with multi-channel radar systems. J. Surv. Mapp. Eng. 1 (1), 1–6.

Nuzzo, L., Leucci, G., Negri, S., Carrozzo, M.T., Quarta, T., 2002. Application of 3D visualization techniques in the analysis of GPR data for archaeology. Ann. Geophys. 45 (2), 321–337.

Pipan, M., Baradello, L., Finetti, I., Forte, E., Prizzon, A., 1999. 2-D and 3-D processing and interpretation of multi-fold ground penetrating radar data: a case history from an archaeological site. J. Appl. Geophys. 41, 271–292.

Pipan, M., Baradello, L., Forte, E., Finetti, I., 2001. Ground penetrating radar study of iron age tombs in southeastern Kazakhstan. Archaeol. Prospect. 8, 141–155.

Piro, S., Goodman, D., Nishimura, Y., 2003. The study and characterization of Emperor Traiano's Villa (Altopiani di Arcinazzo, Roma) using high-resolution integrated geophysical surveys. Archaeol. Prospect. 10 (1), 1–25.

Richards, J.D., 1998. Recent trends in computer applications in archaeology. J. Archaeol. Res. 6 (4), 331–382.

Rosi, M., Bertagnini, A., Landi, P., 2000. Onset of the persistent activity at Stromboli volcano (Italy). Bull. Volcanol. 62 (4–5), 294–300.

Schloderer, G., Bingham, M., Awange, J.L., Fleming, K.M., 2011. Application of GNSS-RTK derived topographical maps for rapid environmental monitoring: a case study of Jack Finnery Lake (Perth, Australia). Environ. Monit. Assess. 180 (1–4), 147–161.

Senechal, P., Perroud, H., Senechal, G., 2000. Interpretation of reflection attributes in a 3-D GPR survey at Vall'e d'Ossau, western Pyrenees, France. Geophysics 65 (5), 1435–1445.

Speranza, F., Pompilio, M., D'Ajello Caracciolo, F., Sagnotti, L., 2008. Holocene eruptive history of the stromboli volcano: constraints from paleomagnetic dating. J. Geophys. Res. 113, B09101.

Staley, D.M., Wasklewicz, T.A., Blaszczynski, J.S., 2006. Surficial patterns of debris flow deposition on alluvial fans in Death Valley, CA using airborne laser swath mapping data. Geomorphology 74, 152–163.

Trinks, I., Johansson, B., Gustafsson, J., Emilsson, J., Friborg, J., Gustafsson, C., Nissen, J., Hinterleitner, A., 2010. Efficient, large-scale archaeological prospection using a true three-dimensional ground-penetrating radar array system. Archaeol. Prospect. 17, 175–186.

Vaughan, C.J., 1986. Ground penetrating radar surveys used in archaeological investigations. Geophysics 51, 595–604.

White, R.E., 1991. Properties of instantaneous seismic attributes. Lead. Edge 10, 26–32.

Zhao, W., Forte, E., Pipan, M., Tian, G., 2013a. Ground penetrating radar (GPR) attribute analysis for archaeological prospection. J. Appl. Geophys. 97, 107–117.

Zhao, W., Tian, G., Wang, B., Forte, E., Pipan, M., Lin, J., Shi, Z., Li, X., 2013b. 2D and 3D imaging of a buried prehistoric canoe using GPR attributes: a case study. Near Surf. Geophys. 11 (4), 457–464.